Improving the Selection of Bases of BRDFs for Appearance Preservation

Fernando Melo Nascimento
Departamento de Computação
Universidade Federal de Sergipe
São Cristóvão – SE, Brazil
Email: nascimentofm@ufs.br

André Britto de Carvalho
Departamento de Computação
Universidade Federal de Sergipe
São Cristóvão – SE, Brazil
Email: andre@ufs.br

Beatriz Trinchão Andrade
Departamento de Computação
Universidade Federal de Sergipe
São Cristóvão – SE, Brazil
Email: beatriz@ufs.br

Fig. 1. Linear combination to approximate Orange BBall with $gcuk5$ basis. Gamma = 2.7, Exposure = 1.0, $\omega_{in} = (60^o, 45^o)$.

***Abstract*—An important step in the appearance preservation of real materials is the analysis of how they interact with light. Since this phenomena happens at a microscopic level, heuristics with different complexity have been developed to capture and reproduce it. In order to minimize sampling efforts, one of these approaches consists in representing the reflectance of a material as a linear combination of a basis of known reflectance functions. To accomplish realistic and efficient representations, this basis must be expressive and contain a reduced number of elements. This work presents three approaches to select such basis. The first one performs an empirical leave-one-out optimization procedure. The other two are based on classical and evolutionary clustering algorithms. To improve clustering results, a new BRDF-oriented fitness function is designed. These approaches are evaluated using NNLS algorithm to estimate sampled materials and a comparison based on numerical precision is performed.**

***Keywords*-BRDF; clustering; appearance modeling; genetic algorithms; linear combination of BRDFs.**

I. Introduction

Appearance preservation is a relevant aspect to be considered when creating 3D models from real data, as it seeks to estimate how materials reflect the incident light under different illumination settings. The first step in the reproduction of what is seen in the real world is the analysis of how different materials interact with light. This interaction can be given in different ways: the material can reflect light, absorb light, and it can display more complex phenomena such as fluorescence or inter-reflection. Thus, for different materials, different models can be used, whose dimensionality and complexity vary depending on the properties of the material to be reproduced.

The interaction between light and a surface can be described by the Bidirectional Reflectance Distribution Function (BRDF) [1]. This function calculates the reflectance of a point p on a surface through the quotient of the exitant radiance emitted by p and the incoming irradiance at this point. The irradiance incidence direction and the radiance emission direction define the four basic parameters of a BRDF: the polar coordinates of these directions, respectively $\omega_{in} = (\theta_{in},\ \phi_{in})$ and $\omega_{out} = (\theta_{out},\ \phi_{out})$.

Many computer graphic applications use BRDFs to reproduce materials from the real world. In film and game industries, BRDFs are used to reproduce special effects and realistic animations. These functions can also be used in the digital preservation of scientific and cultural heritage [2] and during quality inspection of products like metal car panels, lacquers, coats and camouflaging materials[1].

The BRDF of a single material can be measured using a gonioreflectometer [1] or through cameras in an image-based process [3]. These measurements are commonly very accurate and generate realistic BRDFs however, as reflectance values are measured from combinations of incident and exitant directions, the number of samples can be very high. Another recurrent problem during the acquisition of samples is the need of environments with highly controlled illumination settings. The acquisition of a BRDF can take days with a gonioreflectometer, or hours using cameras [4].

In order to minimize sampling efforts, previous works have shown that it is possible to represent a material as a linear combination of a basis of BRDFs [5], [6], [7]. This basis is composed of known BRDFs, and an optimization process is performed to find the coefficients of this combination. As this approach defines the BRDF as a linear combination of existing BRDFs, the results tend to be more stable and present consistent renderings.

An important consideration about a basis of BRDFs is its size. On the one hand, more BRDFs means an increase in representativeness for the basis. On the other hand, estimating

[1]Fraunhofer-Institut für Optronik, Systemtechnik und Bildauswertung. Link: http://www.iosb.fraunhofer.de/servlet/is/14836/

a new BRDF from a large basis means more complex optimization techniques and higher rendering costs. In this context, this work explores new ways of finding bases of BRDFs from a set of known BRDFs. These bases must be chosen aiming at both reducing the number of terms required in the linear combination and improving its overall representativeness.

We propose three new approaches to automatically perform such task. The first one consists in an empirical procedure, based on a systematic selection of BRDFs with highest relevance during the approximation of other materials. The other two adopt classical and evolutionary clustering algorithms and are based on k-medoids and Genetic Clustering for Unknown K (GCUK), respectively. To improve the clustering process, a new BRDF-oriented similarity measure was designed.

Another contribution of this work is a set of experiments to evaluate both the ideal size and the expressiveness of a basis of BRDFs. The first is defined using a clustering validation measure and analysing the empirical approach result. The second is measured by approximating a series of reference materials using Non-Negative Least Squares (NNLS) algorithm. The numerical precision and the rendering quality of these approximations are presented and compared with previous work.

This paper is organized as follows. Section II introduces the technical background, followed by the related works in Section III. Section IV details how to represent a new material from a basis of BRDFs, and Section V presents our approaches to generate a basis from a set of known BRDFs. The experiments and the results are presented in Section VI, and conclusions and suggestions for future work are made in Section VII.

II. Technical Background

A. Clustering

Clustering is an unsupervised data-mining task that aims to divide an input data set into clusters with the following property: members of the same cluster have high similarity, whereas the clusters are very separated from each other. Several algorithms have been developed to perform clustering, some of which specific for particular sets of data. To determine to which cluster an element belongs, similarity measures (fitness functions) are adopted.

One problem with classical clustering algorithms is the obligation of choosing into how many clusters the data set must be divided. Genetic clustering algorithms are capable of finding the optimal quantity of clusters, being an alternative when the approximate number of clusters in a data set is unknown.

1) Clustering validation – Davies-Bouldin index: The Davies–Bouldin index ($DBindex$) is a metric for evaluating clustering algorithms proposed by Davies and Bouldin [8]. This index is a function of the ratio of the sum of within-cluster scatter to between-cluster separation [9]. In other words, it is based on two principles of clustering: clusters should be compact and very separated from each other.

III. Related Work

A. Measured BRDFs

A straightforward way to measure reflectance properties of a material is through a device called gonioreflectometer [10]. The gonioreflectometer is basically composed of a photo-detector and a light source, where the photo-detector measures the light reflected from the light source on a point. This device reaches high-precision results, but it is highly time and resource consuming [4], [11]. To overcome these restrictions, several improvements and alternatives have been proposed in the last decades. Image-based approaches became popular in this context, presenting solutions to reduce acquisition time [1], to improve accuracy [11] and to capture BRDFs of surfaces with a regular shape [12].

Using an image-based method, Matusik et al. collected the reflectance data of 100 isotropic materials using a camera and small spheres of materials such as plastics, metals and fabrics [3]. The collected data is known as MERL data set, as this experiment took place in Mitsubishi Electronic Research Laboratories (MERL).

B. Analytical BRDFs

Ward et al. [1] classified analytical BRDFs models into two main categories: empirical and theoretical. The first group refers to models with (commonly) few simple adjustable parameters designed to fit reflectance of materials. These models normally are not physically plausible, since their derivations are not concerned with physics laws. In some cases, the parameters of these models only control the shape of specular lobe(s). Some models classified in this category are the ones proposed by Phong [13] and Ward [1].

Theoretical BRDF models are designed from a careful derivation in order to produce physically plausible renderings [1]. Reflectance models in this category include Cook-Torrance [14], He et al. [15] and Ashikhmin-Shirley [16]. The models in this category usually generate very realistic representations at the cost of higher complexity.

Brady et al. [17] developed a framework called genBRDF to automatically find new analytical reflectance models. Instead of trying to derive them manually, they used a genetic algorithm to generate reflectance models based on a grammar. According to the authors, the goal is not to replace the human effort of deriving analytical models, but to provide a support tool in the development or improvement of analytical models.

C. Using Analytical BRDFs to Reproduce Measured BRDFs

As noted by Ward [1], to use a analytical BRDF model one must consider fitting its parameters to measurements of actual reflectance data. Ngan et al. [18] used the MERL raw data set to fit the parameters of seven analytical BRDF models through a least squares optimization. They found that, using a single specular lobe, the He et al. [15], Cook-Torrance [14] and Ashikhmin-Shirley [16] models reached smaller errors for most of the 100 isotropic BRDFs. A supplemental document (Ngan et al. [19]) presents the formulations used and the

minimized parameters and errors for each one of the 100 rendered materials.

Bilgili et al. conducted a similar experiment using MERL BRDFs with a few different models, including a new formulation [20]. Their supplemental document (Bilgili et al. [21]) contains the parameters of the 100 rendered materials with 3 specular lobes and the PSNR for each rendered material.

Lensch [5] introduced the idea that the reflectance of a material can be represented by a combination of a basis of BRDFs. In his work, reflection properties were obtained by fitting BRDF models to clustered samples from a 3D model. A linear combination of the resulting set of BRDFs were then used to represent the 3D model appearance.

Häußler [22] and Andrade [7] used clustering to group BRDFs in order to find a basis. This approach assumes that the basis is composed by the most representative elements at each cluster. The basis depends basically on the original set of BRDFs and its expressiveness is improved by the choice of an element per cluster. Both works use on k-means, a technique that requires the number of clusters as input. This way, the decision about how many elements the basis of BRDFs must have is not based on the original set of BRDFs, but on a search for a number of clusters that reduces an error metric.

IV. Representing a New Material from a basis of BRDFs

Once the basis of BRDFs is obtained, it is possible to reproduce the appearance of a new material as a linear combination of this basis (Figure 1). To this end, the basis of BRDFs and samples of this material are used to estimate the coefficients of the linear equation.

An implementation of NNLS algorithm [23] was used to find non-negative values for each coefficient in the linear combination given by Equation 1. This combination represents how material B is approximated by the basis of BRDFs. The non-negative restriction is important when dealing with BRDFs, once light is always additive.

$$a_0 + a_1 M_1 + a_2 M_2 + ... + a_k M_k = B. \quad (1)$$

In this combination, each BRDF M_i with $i \in [1,\ k]$ represents the reflectance of each material in the basis and a_0 is a diffuse Lambertian term coefficient. Each a_i with $i \in [1,\ k]$ represents the contribution of material M_i to approximate the desired material B. The number of terms k is the quantity of BRDFs present in the basis.

The optimization process is performed one time for each RGB channel, once they are independent. The final result is described in Equation 2:

$$B = \begin{pmatrix} a_{0r} + a_{1r} M_{1r} + a_{2r} M_{2r} + ... + a_{kr} M_{kr}. \\ a_{0g} + a_{1g} M_{1g} + a_{2g} M_{2g} + ... + a_{kg} M_{kg}. \\ a_{0b} + a_{1b} M_{1b} + a_{2b} M_{2b} + ... + a_{kb} M_{kb}. \end{pmatrix} \quad (2)$$

It is possible that one or more materials in the basis do not contribute to approximate the appearance of the material B in one or more RGB channels. In this case, the coefficients of those materials are 0 in the respective channels.

V. How to Define a Basis of BRDFs?

This section explores this question in order to present new techniques to define a basis of BDRFs from a set of known BRDFs. As detailed in Section I, the goal is to obtain a expressive and compact basis of BRDFs.

This paper develops two approaches to perform this task. The first one is based on a systematic evaluation of the data set and it is presented in Subsection V-A. The second approach is based on clustering algorithms and assumes that the basis is composed of the most representative elements of each cluster. Subsection V-B compares two different clustering algorithms and present a new fitness function, designed specially to measure similarity between two BRDFs.

A. Empirical Selection of a Basis

An empirical approach was developed to select the materials for a basis using a systematic criteria. Rather than choosing the representative member of a cluster to be in the basis, this approach computes the number of contributions that each material in the data set presents during the approximation of other materials. The procedure can be seen as a leave-one-out method and is described in Algorithm 1.

```
Data: MERL BRDFs data set.
Result: Histogram of contributions of each material.
begin
    Create a histogram contribution array;
    Initialize all positions with value 0;
    foreach element in the data set do
        desired_element := element;
        basis := data set – desired_element;
        Estimate desired_element using basis;
        foreach element in the basis do
            if element contributed to approximate
              desired_element then
                histogram[element] += 1;
            end
        end
    end
end
```

Algorithm 1: Empirical Selection

The resulting histogram can be sorted to easily identify the materials most frequently used in combinations, which are the best candidates to generate a basis of BRDFs. This approach is simple to implement, but it looses performance as the number of elements in the input data set increases.

B. Using clustering techniques

1) K-medoids: K-medoids is a classical hard partitional clustering algorithm based on k-means. Its operation consists of finding k clusters that minimize the distance between members of the same cluster. In contrast with k-means, the

representative element of each cluster is the most centrally located one, being called medoid [8]. A medoid is an actual element of the data set while a k-means' centroid often does not exist, once it is the average of the elements in a cluster.

This algorithm operates on the relation between an overall cost and the distances of elements inside a cluster. The cost is defined as the distance between an element and its cluster's medoid. The overall cost is the sum of all distances calculated.

K-medoids repeatedly exchanges a non-medoid element with its cluster's medoid in order to verify if the overall cost decreases. If so, this modification is saved, otherwise it is reverted. The algorithm stops when the overall cost does not decrease.

The main drawback of k-medoids is the obligation of giving the value of k as input. In many data sets, like the one used in this work, the number of clusters is not known a priori. One strategy to use this algorithm is to variate the value of k and to compare the results.

2) Genetic Clustering for Unknown K: GCUK is an evolutionary clustering algorithm, proposed by Bandyopadhyay and Maulik [9], capable of finding the optimum quantity of clusters in a given data set. The implementation used in this work receives as input the data set and five parameters: the minimum and maximum number of clusters in one solution, the population size, the number of generations and the crossover probability. They are represented, respectively, by k_{min}, k_{max}, P, G_{max} and $Prob_c$.

Each individual in the population represents a possible solution with k_{max} chromosomes. Each chromosome represents a cluster that can be valid if one or more elements are assigned to it, or invalid otherwise. One individual must have at least k_{min} valid chromosomes to be considered valid. If an individual do not meet this restriction, it is discarded.

Crossover operation is performed in two individuals of the population to generate two sons. This step increases the variety of individuals by mixing two different cluster sets to cover a higher space of solutions. Invalid individuals can be generated in this step, as well as sub-optimum solutions.

In selection phase, solutions are sorted by $DBindex$ and selected by roulette to survive for the next generation. Good solutions have higher chances to survive, while sub-optimum individuals have lower chances. All invalid solutions (possibly) generated by crossover are discarded by this operation.

Both genetic operations are applied in the population for G_{max} generations. In the end of the process, the best solution, i. e. with lower value of $DBindex$, is chosen as the result of GCUK. The most centrally located element of each valid chromosome is elected to be its representative.

One important modification from original algorithm is that the mutation step is not performed. The new similarity measure described in Subsection V-B3 expects values referent to real materials. Since mutation operation modifies the original values of materials, it is not suited to the proposed metric. For the same reason k-means algorithm is not indicated to be used, once centroids are not real elements of the data set.

3) A BRDF-oriented Fitness Function – $BRDF_{it}$: Clustering algorithms generally use Euclidean distance as similarity measure. This metric is fast to compute and works well in many general cases, but it tends to generate hyper spherical clusters [8]. There are other fitness functions that can be used in clustering, like Manhattan and Minkowski distance [8], each one with its advantages and disadvantages. Nevertheless, for some data sets the best approach is to develop a specific problem-oriented metric to serve as fitness function.

To deal with BRDF clustering, this paper proposes a new BRDF-oriented fitness function called $BRDF_{it}$ to overcome this issue. The reflectance of a material can be defined using Equation 3, where $\rho_{d[i]}$ and $\rho_{s[i]}$ are, respectively, the diffuse and specular terms of a material i. The incoming and outgoing light directions are represented by ω_{in} and ω_{out} in polar coordinates, respectively.

$$M_{[i]} = \rho_{d[i]}(\omega_{in},\ \omega_{out}) + \rho_{s[i]}(\omega_{in},\ \omega_{out},\ p_{[i]}). \quad (3)$$

The last parameter $p_{[i]}$ in $\rho_{s[i]}$ represents the list of parameters requested by the specular reflectance model of a material i. If raw measured BRDF data is used, the actual reflectance values are given only by ω_{in} and ω_{out}. In this case, it is important to remember that some sampling ranges can be invalid. These ranges represent effects that are not possible to measure due to limitations of the acquisition setup, such as retro-reflection [3].

In many practical applications the diffuse term is assumed to be Lambertian (Equation 4). Once the most relevant differences between BRDFs are generally in their specular reflectances, $BRDF_{it}$ focus only in specular terms.

$$\rho_d(\omega_{in},\ \omega_{out}) = \frac{1}{\pi}. \quad (4)$$

The proposed BRDF-oriented fitness function is based on the mean difference between specular reflectance terms of two materials for each one of q samples of (ω_{in}, ω_{out}). Equation 5 defines this metric for two materials i and j. This metric was designed to be independent from the analytical BRDF model used and also to support measured BRDFs.

$$BRDF_{it[i][j]} = \sum_{\theta_{in}=0}^{\theta_{in}=\frac{\pi}{2}} \sum_{\phi_{in}=0}^{\phi_{in}=2\pi} \sum_{\theta_{out}=0}^{\theta_{out}=\frac{\pi}{2}} \sum_{\phi_{out}=0}^{\phi_{out}=2\pi} \frac{\sqrt{(\rho_{s[i]} - \rho_{s[j]})^2}}{q}. \quad (5)$$

Equation 6 presents the formulation of the specular term of isotropic Ashikhmin-Shirley model [16] adopted in this work. In this equation, H is the halfway angle between L and V, N is the normal vector, $L = \omega_{in}$, and $V = \omega_{out}$.

$$\rho_s(L, V, F_0, n) = \frac{(n+1) \times (N \cdot H)^n \times f(F_0, V, H)}{8\pi \times (V \cdot H) \times max((N \cdot L), (N \cdot V))}. \quad (6)$$

This formulation defines an isotropic exponent n and Schlick's approximation for the Fresnel term, presented in Equation 7. Parameter F_0 represents the reflectance of the material at normal incidence. For this model, the list of parameters $p_{[i]}$ of Equation 3 is composed of F_0 and n.

$$f(F_0, V, H) = F_0 + (1 - F_0) \times (1 - (V \cdot H))^5. \quad (7)$$

VI. Experiments and Results

A series of experiments were performed in both clustering and optimization steps. The data set used in this work is described in Subsection VI-A, followed by the empirical selection experiment in Subsection VI-B. The clustering algorithms executions and their results are presented in Subsection VI-C as well as the selected bases of BRDFs in Subsection VI-D. Finally, Subsection VI-E contains the results of optimization process and renderings.

A. Data set

The experiments performed in this paper use analytical models generated by Ngan et al. [18], [19] for the 100 materials in the MERL data set. As the Ashikhmin-Shirley model consistently outperformed most models regarding fitting quality and representation of real data [18], [20], it is used in the following experiments.

Ngan et al. [18] obtained eight parameters for the Ashikhmin-Shirley model through a least squares optimization. They are: the diffuse RGB values (d_r, d_g, d_b); the specular RGB values (s_r, s_g, s_b); the Fresnel factor (F_0); and an isotropic exponent (n). Only the last two parameters F_0 and n were used in clustering, once the colors of materials can be approximated by a constant Lambertian factor (term a_0 in Equation 1).

B. Empirical Selection – Optimization without Clustering

This experiment uses Algorithm 1 to estimate each of the 100 materials present in MERL data set through a combination of the other 99 materials, using Ashikhmin-Shirley model. The main goals of this experiment are to check the expressiveness of the data set elements and also to estimate the minimum number of elements needed in a basis of BRDFs obtained from MERL data set.

It was observed that all but one material could be approximated through a combination of other 4 or less materials. Polyethylene was the only element that needed 5 materials to be represented, establishing this value as a lower boundary for a basis size. Thus, the minimum number of clusters obtained in the clustering algorithms must be 5.

Figure 2 contains the histogram of contributions observed in this experiment. Each value in the Y-axis represents how many materials contribute to approximate the number of materials in the X-axis. Thus, of all 100 materials in MERL data set, five did not contribute to approximate any other material and most of them were present in five or less combinations. Only 14 contributed to approximate more than five other materials, being the best candidates to be in the basis, once they were more often used in approximations.

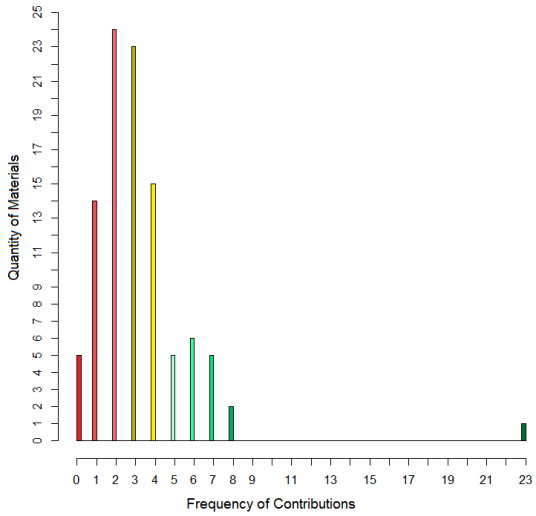

Fig. 2. Histogram of materials contributions in NNLS without clustering.

C. Clustering Algorithms Executions

To overcome the drawback of choosing a fixed value for k as input of k-medoids, an experiment based on the works of Häußler [22] and Carvalho [7] was performed: choosing a range for k. As stated in Section I, a basis of BRDFs must be expressive and yet have few elements. Aiming this end, the lower boundary was established as 5, once it was the number of elements needed to approximate the Polyethylene (VI-B). The maximum value for k was set to 12. This value has been chosen because the clustering quality started to decrease for higher values. These executions were also confronted to the results of GCUK.

K-medoids was executed 30 times for each $k \in [5, 12]$. Also, 30 executions of GCUK were performed with $k_{min} = 5$ and $k_{max} = 20$. The population consisted of 20 individuals tested for 10 generations with 100% of crossover probability to enforce covering a higher solution space. Euclidean distance between the parameters (F_0, n) of each material and $BRDF_{it}$ were compared as fitness functions for each method.

Figure 3 contains two box-plots with $DBindex$ values obtained with the clustering algorithms. Figure 3a shows the results using Euclidean distance, while the values achieved with $BRDF_{it}$ are presented in Figure 3b.

To compare the results of each set of experiments, the Friedman test at 95% significance level was performed. This test indicates if there is any statistical difference between each analyzed data set. Then, the median values and a post-hoc procedure are used to identify which algorithm has the best results. According to the analysis of the statistical test, GCUK obtained the best results among all algorithms, for both Euclidean distance and $BRDF_{it}$.

Furthermore, both versions of GCUK, with Euclidean distance and $BRDF_{it}$, were confronted using Wilcoxon test, again with 95% significance level. For this comparison, the p-value of the test was smaller than $2.2e^{-16}$, which indicates that there is a significant difference between the samples.

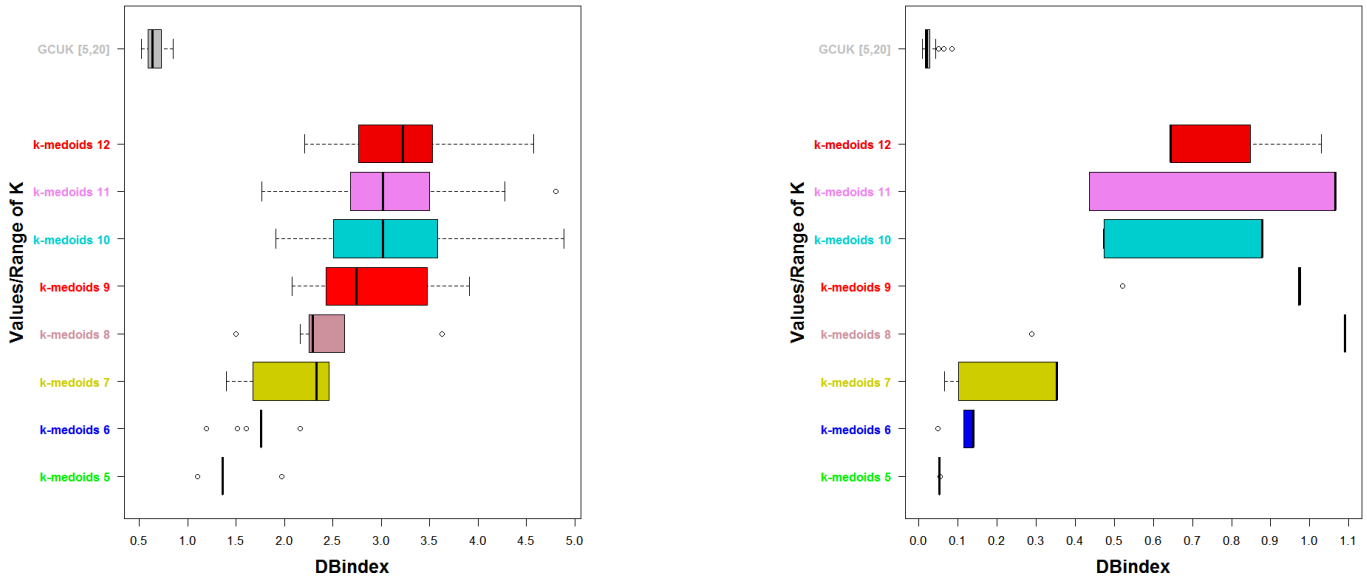

(a) Executions using Euclidean distance

(b) Executions using $BRDF_{it}$.

Fig. 3. Box-plot of $DBindex$ values for k-medoids and GCUK executions.

Observing Figure 3, executions with $BRDF_{it}$ reached smaller $DBindex$ values than the ones with Euclidean distance, implying a better clustering in terms of $DBindex$. Thus, it can be inferred that $BRDF_{it}$ is a better fitness function than Euclidean distance for clustering BRDFs.

D. Novel basis of BRDFs

Five novel basis were selected from previous experiments. Table I contains Ashikhmin-Shirley renderings (taken from Ngan et al. supplemental document [19]) of all materials in each basis. The first one consists of the 14 materials that contributed in more than five combinations in the experiment described in Subsection VI-B. Two bases were generated using k-medoids with $BRDF_{it}$: $kmedoids5$, yielded by the best configuration among all values of k based on $DBindex$, and $kmedoids12$, selected from an execution with $k = 12$, aiming to increase the expressiveness. The last two bases were obtained through GCUK executions, again using $BRDF_{it}$: $gcuk5$ is the result of the best GCUK execution based on $DBindex$ and $gcuk10$ was obtained in the execution with the higher number of clusters founded.

E. NNLS Optimization

To verify the expressiveness of each one of the five bases presented in Subsection VI-D, NNLS algorithm was used to estimate coefficients for these bases in order to approximate a subset of the MERL BRDFs. Only materials that are not present in any basis were included in this subset, totalizing 62 materials. Disney's BRDF Explorer tool [24] was used to render the original materials and their combinations.

Two Mean Absolute Error (MAE) analysis were performed for all 62 materials approximated by each basis. The first one compared reflectance data measurements of each material and their approximations. Data with incident or outgoing angles larger than 80 degrees and samples within 3 degrees from the retroreflection direction were ignored. The second analysis computed the normalized MAE between the images of a rendered material and its' approximations. Figure 4 contains plots of both analysis. Errors are sorted by $gcuk10$ basis.

It can be observed in Figures 4a and 4b that $kmedoids5$ and $kmedoids12$ reached good error values in both analysis. The $empirical$ basis presented an unstable behaviour in the numerical analysis, but had a good performance in renderization analysis. GCUK's bases did not achieve the same success, but still reached acceptable values. Figure 5 contains renderings and heatmap images of Alum Bronze material. In this example $empirical$ basis outperformed the others, reaching better visual results.

VII. Conclusion

This paper presented new ways of choosing bases of BRDFs capable of approximating diverse materials. An empirical method based on the systematic analysis of which materials most appear in a set of possible combinations was proposed to accomplish this goal.

Two clustering techniques were also proposed for selecting a basis of BRDFs: k-medoids and Genetic Clustering for Unknown K – GCUK. A new BRDF-oriented similarity measure, $BRDF_{it}$, was proposed to improve the clustering results of BRDFs sets. $BRDF_{it}$ is independent of the analytical BRDF model chosen and also works with measured data. It is also capable of reducing the $DBindex$ values of both k-medoids and GCUK executions in comparison with the use of Euclidean distance.

Numerical comparisons among five novel bases showed that k-medoids bases outperformed the other ones. Meanwhile,

TABLE I
NOVEL BRDFS-BASES

Bases	Materials						
empirical	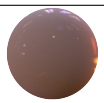 Acr. White	 B. O. Steel	 B. P. Soft	 Blue Rubber	 G. Metallic	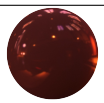 R. Metallic	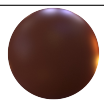 Col. Mapple
	 Fab. Beige	 Natural 209	 Nickel	 Pickled Oak	 Pink Plas.	 R. F. Wax	 R. Quartz
*kmedoids*5	 Acr. Blue	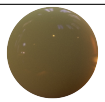 Acr. Yellow	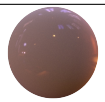 Alu. Oxide	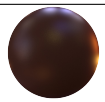 Cherry 235	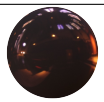 Steel		
*kmedoids*12	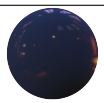 Acr. Blue	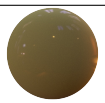 Acr. Yellow	 Black Obsi.	 B. O. Steel	 Chrome	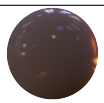 Gray Plas.	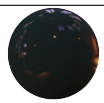 Green BB.
	 Green Plas.	 Maroon BB.	 Sil. Nitrade	 Steel	 Sugar		
*gcuk*5	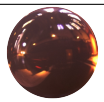 Copper	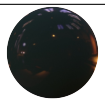 Green BB.	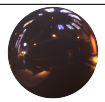 Hematite	 Pink Plas.	 Red. P. Spc.		
*gcuk*10	 Acr. Green	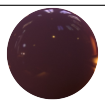 Acr. Violet	 Black Ph.	 Fab. Beige	Fab. Black	Fruit. 241	Ph. Yellow
	Pink Jasper	PVC	Sil. Nitrade				

it was observed that the empirical basis also yields good rendering results.

The use of different clustering validation metrics and genetic optimization techniques are proposed as future work. The first aims the confirmation of the clustering results, while the second can improve the approximation step.

Other directions are: plot the BRDFs specular lobes as addition to MAE analysis, rerun experiments with measured raw data and improve $BRDF_{it}$ to observe the Jacobian change of variables from directions to spherical coordinates.

ACKNOWLEDGMENTS

A special thanks goes to Mislene da Silva Nunes for the technical support. The authors would also like to thank COPES/UFS for the financial support during this research (project PIBIC PVB3851-2015).

REFERENCES

[1] G. J. Ward, "Measuring and Modeling Anisotropic Reflection," *SIGGRAPH Comput. Graph.*, vol. 26, no. 2, pp. 265–272, Jul. 1992.

[2] B. T. Andrade, C. M. Mendes, J. d. O. Santos, O. R. P. Bellon, and L. Silva, "3D Preserving XVIII Century Barroque Masterpiece: Challenges and Results on the Digital Preservation of Aleijadinho's Sculpture of the Prophet Joel," *Journal of Cultural Heritage*, vol. 13, no. 2, pp. 210–214, 2012.

[3] W. Matusik, H. Pfister, M. Brand, and L. McMillan, "A Data-Driven Reflectance Model," in *Computer Graphics (SIGGRAPH 2003 Proceedings)*, vol. 22, no. 3, 2003, pp. 759–769.

[4] T. Weyrich, J. Lawrence, H. P. A. Lensch, S. Rusinkiewicz, and T. Zickler, "Principles of Appearance Acquisition and Representation," *Found. Trends. Comput. Graph. Vis.*, vol. 4, no. 2, pp. 75–191, 2009.

[5] H. P. A. Lensch, "Efficient, Image-Based Appearance Acquisition of Real-World Objects," Ph.D. dissertation, Universität des Saarlandes, 2003.

[6] R. P. Weistroffer, K. R. Walcott, G. Humphreys, and J. Lawrence, "Efficient basis decomposition for scattered reflectance data," in *EGSR07: Proceedings of the Eurographics Symposium on Rendering*, June 2007.

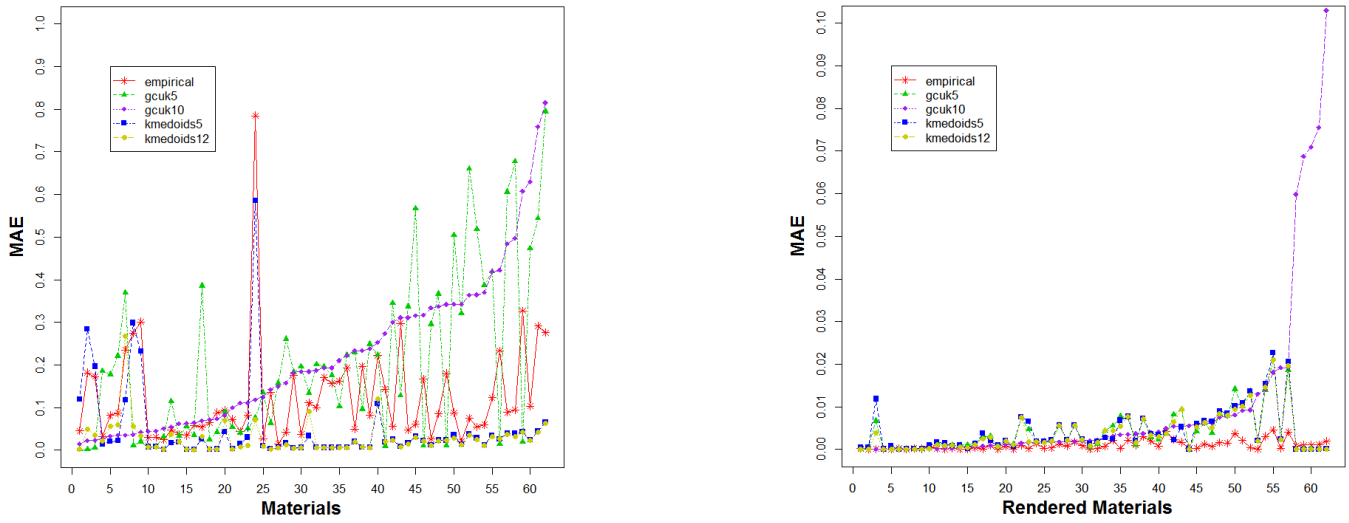

(a) Data measured errors

(b) Normalized image errors

Fig. 4. Mean Absolute Errors for all 62 materials approximated by each basis of BRDF.

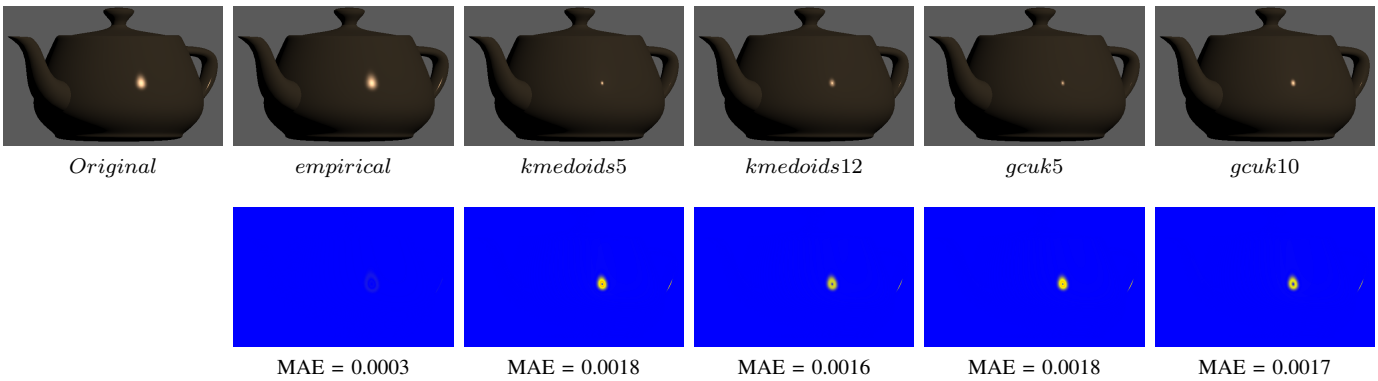

Fig. 5. Alum Bronze renderings, heatmaps and normalized image Mean Absolute Errors. Gamma = 2.2, Exposure = 0, $\omega_{in} = (45^o, 45^o)$.

[7] B. T. Andrade de Carvalho, "Image-Based Appearance Preservation," Ph.D. dissertation, Universidade Federal do Paraná, 2013.

[8] R. Xu and D. Wunsch, II, "Survey of Clustering Algorithms," *Trans. Neur. Netw.*, vol. 16, no. 3, pp. 645–678, May 2005.

[9] S. Bandyopadhyay and U. Maulik, "Genetic Clustering for Automatic Evolution of Clusters and Application to Image Classification," *Pattern Recognition*, vol. 35, no. 6, pp. 1197–1208, 2002.

[10] J. J. Hsia and J. C. Richmond, "A High Resolution Laser Bidirectional Reflectometer With Results on Several Optical Coatings," in *National Bureau of Standards*, 1976.

[11] D. R. White, P. Saunders, S. J. Bonsey, J. van de Ven, and H. Edgar, "Reflectometer for measuring the bidirectional reflectance of rough surfaces," *Appl. Opt.*, vol. 37, no. 16, pp. 3450–3454, Jun 1998.

[12] S. Marschner, S. Westin, E. Lafortune, K. Torrance, and D. Greenberg, "Image-Based BRDF Measurement Including Human Skin," in *Eurographics Workshop on Rendering*, 1999, pp. 131–144.

[13] B. Phong, "Illumination for Computer Generated Pictures," *Communications of the ACM*, vol. 18, no. 6, pp. 311–317, 1975.

[14] R. Cook and K. Torrance, "A Reflectance Model for Computer Graphics," *ACM Transactions on Graphics*, vol. 1, no. 1, pp. 7–24, 1982.

[15] X. He, K. Torrance, F. Sillion, and D. Greenberg, "A Comprehensive Physical Model for Light Reflection," *Computer Graphics (SIGGRAPH '91 Proceedings)*, vol. 25, no. 4, pp. 175–186, 1991.

[16] M. Ashikhmin and P. Shirley, "An Anisotropic Phong BRDF Model," *Journal of Graphics Tools*, vol. 5, no. 2, pp. 25–32, 2000.

[17] A. Brady, J. Lawrence, P. Peers, and W. Weimer, "genBRDF: Discovering New Analytic BRDFs with Genetic Programming," *ACM Trans. Graph.*, vol. 33, no. 4, pp. 114:1–114:11, jul 2014.

[18] A. Ngan, F. Durand, and W. Matusik, "Experimental Analysis of BRDF Models," in *Eurographics Symposium on Rendering*. Eurographics Association, 2005, pp. 117–126.

[19] ——, "Experimental Analysis of BRDF Models - Supplemental," 2005.

[20] A. Bilgili, A. Öztürk, and M. Kurt, "A General BRDF Representation Based on Tensor Decomposition," *Comput. Graph. Forum*, vol. 30, no. 8, pp. 2427–2439, 2011.

[21] ——, "A General BRDF Representation Based on Tensor Decomposition: Supplemental Material," 2011.

[22] T. Häußler, "Mobile Reflectance Estimation," Master's thesis, Universität Ulm, Fakultät für Ingenieurwissenschaften und Informatik, 2012.

[23] V. Oikonen, "nnls.c File Reference. Finnish National Research Institute," 2013.

[24] Disney, "BRDF Explorer Tool," [web page] http://www.disneyanimation.com/technology/brdf.html, 2016.